Biophysical Journal Volume 100 June 2011 2955–2963


# Transmembrane Signaling of Chemotaxis Receptor Tar: Insights from Molecular Dynamics Simulation Studies

Hahnbeom Park,[†] Wonpil Im,[‡] and Chaok Seok[†*]
[†]Department of Chemistry, Seoul National University, Seoul, Republic of Korea; and [‡]Department of Molecular Biosciences and Center for Bioinformatics, The University of Kansas, Lawrence, Kansas

ABSTRACT Transmembrane signaling of chemotaxis receptors has long been studied, but how the conformational change induced by ligand binding is transmitted across the bilayer membrane is still elusive at the molecular level. To tackle this problem, we carried out a total of 600-ns comparative molecular dynamics simulations (including model-building simulations) of the chemotaxis aspartate receptor Tar (a part of the periplasmic domain/transmembrane domain/HAMP domain) in explicit lipid bilayers. These simulations reveal valuable insights into the mechanistic picture of Tar transmembrane signaling. The piston-like movement of a transmembrane helix induced by ligand binding on the periplasmic side is transformed into a combination of both longitudinal and transversal movements of the helix on the cytoplasmic side as a result of different protein-lipid interactions in the ligand-off and ligand-on states of the receptor. This conformational change alters the dynamics and conformation of the HAMP domain, which is presumably a mechanism to deliver the signal from the transmembrane domain to the cytoplasmic domain. The current results are consistent with the previously suggested dynamic bundle model in which the HAMP dynamics change is a key to the signaling. The simulations provide further insights into the conformational changes relevant to the HAMP dynamics changes in atomic detail.

## INTRODUCTION

Motile bacteria respond to chemical gradients and move toward areas of favorable chemical environment. This so-called chemotaxis is triggered by binding of attractant or repellant molecules to chemotaxis receptors. These receptors regulate cytoplasmic histidine kinases that eventually lead to modulation of the flagella motion. The chemotaxis pathway constitutes a relatively simple system and is highly conserved in prokaryotes. Chemoreceptors form homodimers with four modulated domains (Fig. 1). The periplasmic domain initiates signaling upon binding of a ligand. Two helices from each chain of the periplasmic domain continue in the bilayer membrane to form the transmembrane (TM) four-helix bundle. The two TM helices (each from different monomers) are connected to the cytoplasmic domain by a linker, called the HAMP domain. The HAMP domain is a widespread signaling motif found in a variety of bacterial proteins (1). This domain converts signals from the TM helices into responses at the cytoplasmic domain (1).

Extensive experimental studies on chemoreceptors have revealed important mechanistic features of chemoreceptor signaling, as reviewed in (2–4). Until now, a number of different transmembrane signaling mechanisms have been suggested for chemoreceptors. Many experiments (5–9) support the piston-motion mechanism (10,11), in which the signal is transmitted across the membrane and all the way to the helices at the cytoplasmic domain by continuous piston motions. Despite the clear evidences for the piston motion at the periplasmic domain (12), whether such a motion exists across the membrane is elusive; only indirect clues have been reported by mutation studies (8,9). Moreover, how this movement induces conformation changes at the HAMP domain remains unresolved. Many experiments focused on the HAMP domain have suggested various models for the signaling mechanism including the gearbox-model (13), the dynamic-bundle model (14), and the scissor-like motion model (15). In addition, the importance of the short linker called the control cable that connects the TM helices to the HAMP domain was recently noticed (1), but how this linker is involved in the signaling process is still unknown. Related to the signaling mechanism, it is also not clearly understood why ligand binding at one of the binding sites is preferred to binding at both sites, which is known as negative cooperativity (16,17).

Most previous studies focused on either the periplasmic domain (5–7,11) or the HAMP domain (14,18,19) and thus our understanding of the TM domain are relatively limited because of experimental difficulties with membrane proteins. Although several experiments were performed on the TM domain (8,9), such methods have limited resolution in identifying potential asymmetric changes in the homodimeric TM helices, which are supposedly induced by the asymmetric piston motion upon ligand binding to one of the periplasmic binding sites. Therefore, computational modeling/simulation studies on this system, together with available experimental data, could have potential advantages in elucidating the detailed TM-TM and TM-lipid interactions during the signaling process. About a decade ago, a computational study on transmembrane signaling of chemoreceptors was reported using a simple modeling

*Submitted March 21, 2011, and accepted for publication May 12, 2011.*
*Correspondence: chaok@snu.ac.kr
Editor: Benoit Roux.

0006-3495/11/06/2955/9 $2.00
doi: 10.1016/j.bpj.2011.05.030

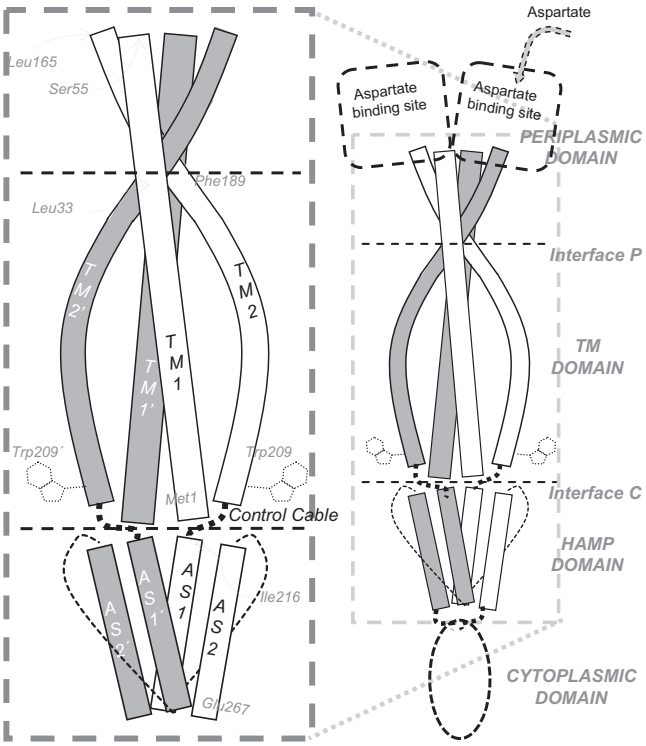


FIGURE 1 Schematic representation of the simulated system. The homodimeric units are colored in white and gray, respectively. Notations for the structural units and the ranges of the residues that compose the units are shown together. The periplasmic and cytoplasmic domains not included in the simulations are indicated with a box and an oval at the top and bottom, respectively. The membrane-water interfaces at the periplasmic side (interface P) and at the cytoplasmic side (interface C) are shown as dashed lines.

scheme and limited molecular dynamics (MD) simulations (20). Surprisingly, to the best of our knowledge, no other computational studies were reported on chemoreceptor transmembrane signaling, including the TM domain, most likely due to the lack of an entire chemoreceptor structure.

In this work, the transmembrane signaling of the chemotaxis aspartate receptor Tar from *Salmonella typhimurium* is studied by advanced MD simulation techniques (21,22) together with experimental information. We carried out a total of 600-ns comparative MD simulations (including model-building simulations) of Tar (a part of the periplasmic domain/TM domain/HAMP domain) in explicit lipid bilayers. By performing restrained MD simulations (based on experimental information) coupled with simulated annealing, stable models of the TM domain are constructed. The NMR structure of HAMP from a thermophile protein Af1503 (13) is then connected to the TM models and simulated together with a part of the periplasmic domain that mimics either the ligand-off or ligand-on state. These simulations reveal valuable insights into the mechanistic picture of the Tar transmembrane signaling; the piston-like movement of a TM helix induced by ligand binding on the periplasmic side is transformed into a combination of both longitudinal and transversal movements of the helix on the cytoplasmic side as a result of different protein-lipid interactions in between ligand-off and ligand-on states of the receptor. This conformational change alters the dynamics and conformation of the HAMP domain, which is presumably a mechanism to deliver the signal from the TM domain to the cytoplasmic domain. The current results are consistent with the previously suggested dynamic bundle model in which the HAMP dynamics change is a key to the signaling. The simulations provide further insights into the conformational changes relevant to the HAMP dynamics changes in atomic detail.

## METHODS

### Simulation systems

A homodimer system of Tar was made up of two identical monomers, each of which consists of 158 amino acids, with the full TM and HAMP domains and a part of the periplasmic domain connected to the TM region (Fig. 1). The periplasmic domain residues connected to TM was included not only to have a realistic TM domain with the four-helix bundle, but also to take into account the ligand-off and ligand-on states. The crystal structures of the periplasmic domain from *S. typhimurium* Tar (12) and the NMR structure of the HAMP domain from a thermophile protein Af1503 (13) were used as initial structures for the corresponding domains. The TM domain structure has not been determined yet and was modeled on the basis of the TM sequence of *S. typhimurium* Tar (UniProt database accession ID: P02941) as well as available experimental data (see below). Cells expressing the chimeric Tar with Af1503 HAMP were responsive to attractant stimuli but did not show effective chemotaxis (13). Therefore, the current simulations may not show the full conformational changes necessary for effective function especially near HAMP, but the observed changes may still provide insights into the mechanism of chemotaxis receptor transmembrane signaling.

The following two states of Tar were simulated: a ligand-off state in which both periplasmic ligand binding sites are free (apo-apo or AA) and a ligand-on state in which a ligand is bound to one of the binding sites (apo-holo or AH). The AH state is known to be preferred to the state with two ligands bound to both sites (holo-holo or HH), showing negative cooperativity (16,17). The crystal structures of the periplasmic domain are available for the AA state (Protein Data Bank (PDB) code 1VLS) and the HH state (PDB code 1VLT) (12), but not for AH. A model for AH was built by superimposing the monomer structure (Ser-55-Asp-142) of PDB:1VLS onto PDB:1VLT (see Fig. S1 in the Supporting Material). Note that the periplasmic helix from Thr-154 to the C-terminal connected to TM2 was not included during the structure superimposition because a major structural change occurs in this helix while the overall structure is well maintained (6,7), as shown in Fig. S1. Because it is computationally too costly to use the entire periplasmic domain and this study aims to study the signal transmission from the periplasmic domain to the TM/HAMP domains, we used the spatial restraints for the periplasmic side of the TM domain instead of simulating the entire periplasmic domain explicitly. The spatial restraints for the residues shown in Fig. S1 were extracted from these superimposed structures to effectively account for the structural change in the periplasmic domain induced by ligand binding. Throughout this work, the residues and structural units of the ligand-on monomer in AH and the corresponding monomer in AA are indicated by a prime, e.g., Trp-209′ or TM2′.

### Model building and MD simulations

The overall procedure to build and simulate the AA and AH models is summarized in Table S1, in the Supporting Material. For the TM domain,

the restraints derived from the disulfide cross-linking experiment (23) and the restraints for maintaining the helical conformation were applied. For the periplasmic domain near the TM terminus, as described above, the restraints were obtained by the superimposition of two periplasmic crystal structures: PDB:1VLS (AA) and PDB:1VLT (HH). Detailed information on these restraints is given in Table S1 and S2.

First, all-atom models for the AA and AH states were generated with MD simulations in the GBSW implicit membrane (24) using the CHARMM program (25). The CHARMM27 force field (26) was used. Temperature was set to 300 K using Langevin dynamics. All bonds involving hydrogen were constrained using SHAKE (27), allowing a 2-fs integration time. Initial 1-ns simulation of four ideal TM helices of polyalanine was performed by gradually increasing the restraint force constants (Table S1). The purpose of this stage was to generate reasonable initial TM models (in implicit membrane) for the following all-atom model-building simulation (in explicit membrane); n. b., such TM modeling from dissociated helices is difficult in explicit bilayers. At this stage, the HAMP domain was not attached to the TM helices explicitly, but temporary conformational restraints at the control cable derived from the NMR structure of HAMP describing its connection to TM2 were applied. The control cable corresponds to five residues (Gly-211 to Thr-215) right after Trp-209 of TM2 at the cytoplasmic side of the receptor. Note that the control cable in the initial structure based on the HAMP NMR structure was in an $\alpha$-helical conformation, and this part remained $\alpha$-helical at this stage. After placing the native side chains using SCWRL 3.0 (28), a 4-ns simulation was carried out by gradually increasing the restraint force constants. Additional 1-ns simulation was then performed after attaching the HAMP domain based on the control cable conformation.

Next, the model-building MD simulations of the AA and AH states were performed in explicit lipid bilayers using GROMACS (29). The SPC water (30) and the united atom lipid model (31) were used with the GROMOS87 force field peptide parameter (32). A lipid bilayer with 128 DPPC (dipalmitoylphosphatidylcholine) molecules (33) was constructed at first. The Tar TM domain covers a small area of the lipid bilayer, and distances between the periodic images of the protein are >20 Å. Initial protein position along the bilayer normal was adjusted by matching the interface residues (such as Val-7, Leu-33, Phe-189, and Ser-213) predicted on UniProt (34) with the lipid hydrophobic region. Lipids that are within 1.0 Å to the protein atoms were then removed. Simulation boxes for AA and AH were prepared separately, resulting in 46,508 atoms including 100 DPPC molecules and 12,696 SPC waters in AA, and 46,290 atoms including 98 DPPC molecules and 12,802 SPC waters in AH. Equilibration of water and lipid molecules was first carried out for 5 ns by fixing protein atoms. The whole system was then replicated to five independent systems (for each of the AA and AH) with different initial velocity assignments. Each of the systems was subjected to a 50-ns simulation by gradually decreasing the restraint force constants (Table S1).

Similarities between the AA and AH models obtained from independent simulations were measured by the common contacts (see Table S3 for details). Similarities among the same state models were higher than those between different states except for a single simulation for AH. We selected a representative model for each of the AA and AH and used it as the initial structure for the 120-ns MD production simulations. Three independent MD simulations of 120 ns were carried out with each representative model by assigning different initial velocities, keeping only the restraints for the periplasmic domain to take into account its structural change upon ligand binding. Trajectories were collected every 1 ps and the final 100-ns trajectories were used for analyses.

The identical simulation parameters were applied for the model building and subsequent MD simulations using GROMACS. The simulations were executed by coupling each system to the Berendsen thermostat (35) at 323 K with the coupling constant of 0.1 ps and to the semiisotropical Berendsen barostat (35) at 1 bar with the coupling constant of 1 ps and compressibility of $4.5 \times 10^{-5}$ bar$^{-1}$. Electrostatic interactions were calculated with the particle mesh Ewald method (36) with a mesh size of ~1.2 Å for fast Fourier transformation, and van der Waals interactions were calculated with the cut-off distance of 12 Å. All bonds with hydrogen were constrained with the LINCS algorithm (37) and the 2-fs integration time was used.

## RESULTS AND DISCUSSION

### Stability and validation of the Tar models

The stability of the model structures of the chemotaxis aspartate receptor Tar from *S. typhimurium* was first examined by the $C_\alpha$ root mean-square deviations from the initial structures as a function of time. As shown in Fig. S2, the model structures mostly remain within 3 Å from the initial structures of the ligand-off (AA) and ligand-on (AH) states during the entire simulation time including the model-building simulations. The trajectories can therefore be considered relatively stable for the long helical bundle structure with 316 amino acids.

Consistency of the models with the disulfide cross-linking experiment (23) was also checked. Because the disulfide cross-linking restraints were applied in the model-building stage and removed afterward, it is worthwhile to examine whether the residues that can be cross-linked in experiment are close enough in the 120-ns trajectories. However, it is not clear if the cross-linking data correspond to the AA or the AH state (23) and it could possibly correspond to a mixture of both states. Assuming that an instantaneous contact is enough for disulfide bond formation, 28 of the 34 residue pairs in Table S2 have the $C_\beta$-$C_\beta$ distance within 5 Å, and all of them are within 5.8 Å (Fig. S3). Although the canonical $C_\beta$-$C_\beta$ distance for a disulfide bond is <4.6 Å, a distance of ~5 Å or slightly larger in the simulations may correspond to the cross-linking distances in the experiment, considering the packing difference of Cys residue substitutions used in the experiment and the wild-type residues in the current simulations.

### Structural characteristics of the Tar models

The Tar TM domain shows a coiled-coil structure with four $\alpha$-helices, twisted clockwise about the supercoil axis (Fig. 2). The two helices in each monomer are denoted by TM1 and TM2 or by TM1′ and TM2′; n. b., the residues and structural units of the ligand-on monomer in AH and of the corresponding monomer in AA are indicated by a prime. The Tar TM structure is clearly distinct from the typical coiled-coil packing with heptad repeats. Near the lipid-water interface on the periplasmic side (referred to as interface P), the four helices are packed tightly, as suggested in the previous disulfide cross-linking study (23). At the bilayer center, TM1 and TM1′ approach each other closely, which is maintained by hydrogen bonds between embedded polar residues, Gln-22 and Ser-25 (Fig. S4 *A*). These polar residues were recognized to be important for dimerization of Tar in a mutation study (38). By contrast, TM2 and TM2′ are

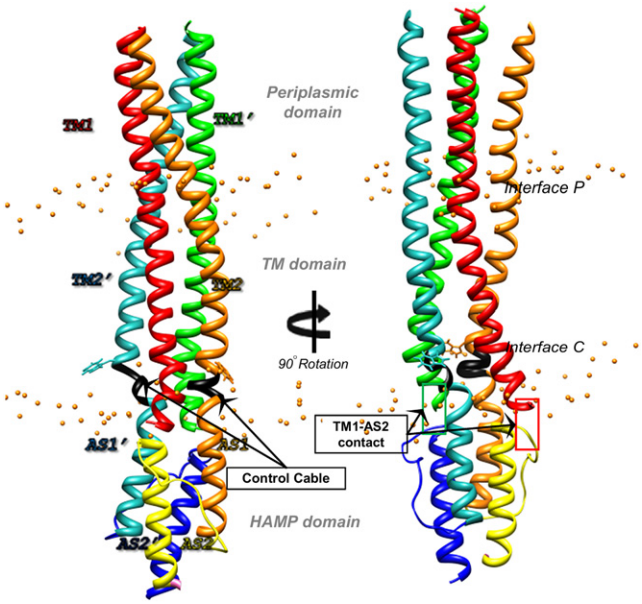


FIGURE 2 Average structure for the AA state obtained from the simulation A is shown from two viewpoints rotated by 90°. DPPC phosphorus atoms are represented as orange spheres to show the water-membrane interfaces. Notations for the helices in the TM domain (TM1, TM1′, TM2, and TM2′) and for those in the HAMP domain (AS1, AS1′, AS2, and AS2′) are shown along with the structure on the left. The control cables that connect TM2 and AS1 are colored in black. The side chains of Trp-209 and Trp-209′ located right above the control cable is explicitly shown.

slightly bent out from the TM1 core at the bilayer center. Near the lipid-water interface on the cytoplasmic side (referred to as interface C), TM2 and TM2′ come close to form a core, and TM1 and TM1′ bend out slightly. The closest $C_\alpha$-$C_\alpha$ distances between TM1-TM1′ of the average AA structure at the interface P, bilayer center, and interface C are 7.3, 7.5, and 15.1 Å, respectively, whereas the TM2-TM2′ distances are 11.5, 15.9, and 7.6 Å, respectively. This unusual TM packing in Tar appears to be an optimal design for transmembrane signaling, as discussed below.

Near the interface C, tryptophan residues (Trp-209 on TM2 and Trp-209′ on TM2′) stretch their aromatic side chains outward from the core, as shown in Fig. 2. These flanking Trp residues are known to be essential for Tar signaling (8,9), contributing to anchoring of Tar at a specific location inside the membrane by favorable protein-lipid interactions, as observed from a mutation study on other transmembrane proteins (39). Several residues near the interface C that come right after Trp-209 compose a special region called the control cable (*black* in Fig. 2). In our simulations, the control cable is mainly positioned at the intermediate region between the hydrophobic core and the head group in the lipid bilayer (Fig. S5). This observation may help us to understand that there exist two contradictory views on the position of the control cable (9,40) depending on whether the intermediate region is considered as a part of the hydrophobic core or a part of the polar head group in lipid bilayer. In the average MD structures, the control cable forms a rather flexible local structure that is slightly different from the initial canonical α-helix (see Methods). As the control cable connects TM2 and AS1 of the HAMP domain, a signal transfer through the membrane may be strongly affected by its structural flexibility, as discussed below.

Another interesting feature in the model structure is the interactions between the TM1 N-terminal residues and the HAMP AS2 N-terminal residues, as shown in Fig. S4, *B–E*, and also summarized in Table S4. These results seem to suggest that the TM1 tail on the cytoplasmic side may also participate in the HAMP domain modulation, as TM2 does. However, previous studies on TM1 N-terminus (41) and on HAMP (42) showed that a wide variety of mutations on these regions could be tolerated with no loss of function, suggesting that this interaction is not an essential functional feature of Tar.

## Piston displacement of TM2′ is transmitted across the membrane by delicate conformational changes

To explore how the piston displacement at the periplasmic domain induced by ligand binding is transmitted across the membrane, we examine the differences in the simulation results for the AA and AH states. When the average structure of the AH state is compared with that of AA, TM2′ in AH shows a longitudinal displacement perpendicular to the membrane compared to TM2 near the interface P (Fig. 3 *a*). Such asymmetric displacement is absent in AA. In addition, AS1′ in AH, which is connected to TM2′, shows a similar movement against AS1 near the interface C (see Fig. 3 *c*). The magnitudes of such asymmetric displacements measured at Thr-179′ (near the interface P) and Ile-220′ (near the interface C) are 1.1 ± 0.7 Å and 1.8 ± 0.4 Å, respectively, as summarized in Fig. S6; although the absolute magnitudes are small, they are statistically significant and three independent simulations show the consistent results.

The longitudinal displacement of TM2′ near the interface P is natural because the helix in the periplasmic domain that undergoes a piston displacement upon ligand binding, mimicked by the restraints (see Methods), continues with TM2′. However, how is the longitudinal displacement of TM2′ at the interface P delivered to that of AS1′ in HAMP at the interface C? A simple sliding of TM2′ along the bilayer would cause hydrophobic mismatch, but lipid adaptation would be harder in this system because the lipid bilayer is already thicker than usual near the protein to reduce a possible hydrophobic mismatch due to the longer TM helices of 25 to 27 residues, as seen in Fig. 2. This fact suggests that a different kind of motion than a simple sliding may be preferred in the Tar TM domain. To explore the relay of the TM2′ piston displacement through the

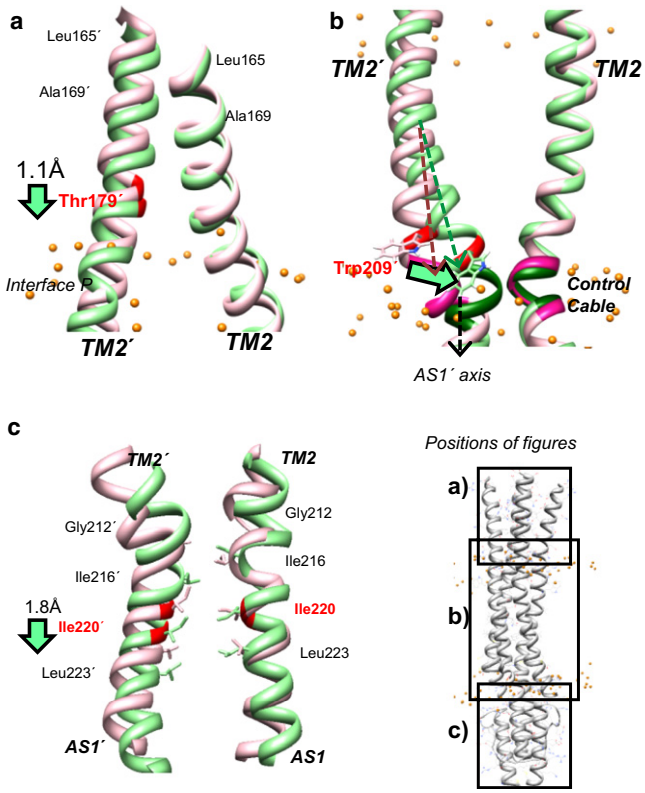


FIGURE 3 Average structures of AA (*pink*) and AH (*green*) in (*a*) the lipid-water interface on the periplasmic side (interface P), (*b*) the TM region, and (*c*) the lipid-water interface on the cytoplasmic side (interface C), as indicated in the figure on the lower right corner. The spatial restraints from the crystal structure of the periplasmic domain are applied to the periplasmic terminal residues (Leu-165 to Ala-169), the top of helices in *a*. Downward piston movement of TM2′ in the AH state is observed in both *a* and *c*. However, in the TM region shown in *B*, TM2′ undergoes different motions than simple downward sliding. The conformational change of TM2′ upon ligand binding is coupled with the change at the control cable, as shown with darker colors in *b*. The TM2′ axis in the AH state (*green arrow* in *b*) becomes better aligned to the AS1′ axis than that in the AA state (*purple arrow* in *b*). The extents of the TM2′ movements are reported in Table S5 and Figs. S5 and S6.

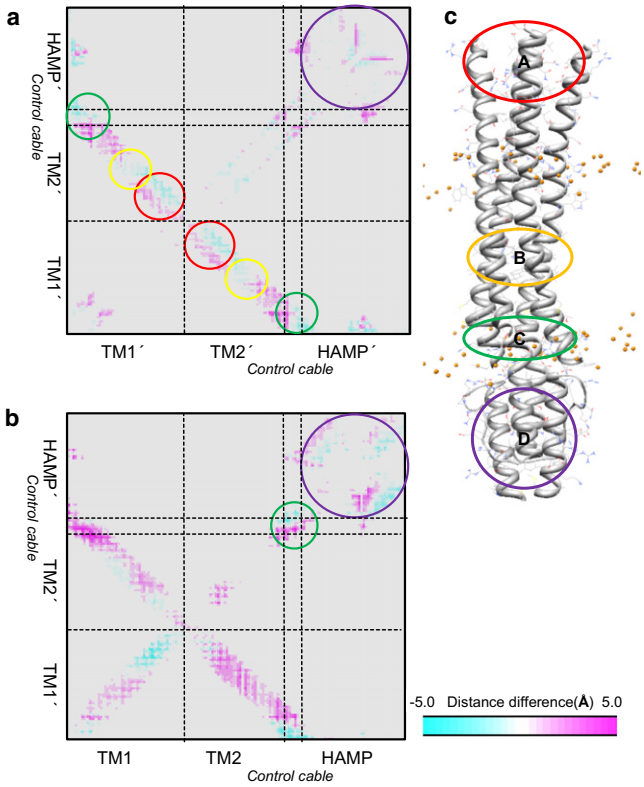


FIGURE 4 Contact map differences between AA and AH from the MD average structures. Cyan spots correspond to residue pairs closer in AA than in AH, and magenta spots the opposite. Only the residue pairs within 15 Å in either AA or AH are considered. The regions with large differences are highlighted by the circles with different colors in the figure on the right. (*a*) The contact difference for the monomer that ligand binds. Prominent changes at the TM1′-TM2′ interface along the inverse-diagonal direction (see *colored circles*) support discontinuous longitudinal movement of TM2′ against TM1′. (*b*) The contact difference for the dimer interface. Sliding of AS1′ relative to AS1 is detected, as shown with a green circle.

membrane, the distances of the Trp-209 residues from the interface C were examined. Strikingly, as shown in Fig. 3 *b* and Table S5, the longitudinal positions of Trp-209 and Trp-209′ are unchanged, suggesting the protein-lipid interactions at the interface C are similar and well maintained for both the AA and AH models. To confirm this unusual movement of TM2′, differences in the residue-residue contact maps of the AA and AH structures were also examined and the results are shown in Fig. 4. Note that the positive value (*magenta*) in Fig. 4 *a* indicates that the distance of the corresponding residue pair is larger in the AA state compared to the AH state. Clearly, the longitudinal displacement of TM2′ relative to TM1′ observed near the interface P (*red circles*) disappears at the bilayer center (*yellow circles*), but reappears clearly near the interface C (*green circles*); n.b., a mixture of magenta and cyan in red and green circles is a hallmark of the longitudinal displacement. These observations suggest that even though the TM2′ piston displacement at the interface P is delivered to a displacement of similar direction and magnitude in HAMP AS1′ at the interface C, TM2′ undergoes more complicated movements than a simple sliding to maintain the favorable protein-lipid interactions.

An apparent change in TM2′ observed near the bilayer center is its bending, as shown in Fig. 3 *b*. TM2′ at the AH state is more bent than TM2 of AH or TM2/TM2′ of AA by ~10°, as summarized in Fig. S7. Fig. 3 *b* also shows the TM2′ bending results in a transversal movement of Trp-209′ along the membrane plane, bringing the two control cables ~2 Å closer from 9.9 Å (standard error 0.7 Å) in AA state to 7.8 Å (standard error 0.2 Å) in AH state at Gly-212, the residues facing each other. The approaching of the control cables in turn largely influences their conformation. This conformational change of the control cable is discussed in more detail below.

## Piston displacement induces rigidity change of the control cable and side chain packing in the HAMP domain

Because the TM domain and the HAMP domain are mainly composed of long $\alpha$-helices, the more rigid the control cable becomes, the more sensitive and effective the control cable will be in reacting to the conformational change in the TM domain. The control cable can be rigidified by becoming more helical. The control cable connected to TM2′ maintains torsion angles of (initial) $\alpha$-helical conformations with much less fluctuations in the AH state than in the AA state. The backbone torsion angles of TM2′ and the control cable are plotted in Fig. S8, and the structures of the control cable are shown in Fig. 3 *b*; the helicity of the control cable is 42% (AH) and 41% (AA) in the initial structures after 50-ns model-building simulations and becomes 46% (AH) and 32% (AA) in the last 50-ns production runs. The standard errors of the helicity among the three independent simulations are 0.30% (AH) and 0.72% (AA), suggesting its statistical significance and convergence. Therefore, the control cable can act as a conformational switch upon ligand binding by changing its rigidity; n.b., the control cable was initially modeled as $\alpha$-helical conformations for both AA and AH states (see Methods). Increased rigidity of the control cable in the AH state can also be seen from the decrease in the root mean-square fluctuation (RMSF) in this region, as shown in Fig. S9. The rigidity change of the control cable has also been suggested to be crucial for the modulation of transmembrane signal in recent studies (1,14), but explanation of this change at the atomistic level was not provided previously. The importance of maintaining the marginal helicity of 30~40% seems to be supported by recent mutation results (43) in which moderate changes to the control cable (length changes of one residue or substitution with poly-Gly of the same length) kept the function of Tar, but larger changes did not. In other words, the control cable should not be fully helical or completely unstructured; if it is fully helical, moderate changes in length or helical propensity would cause malfunction, and if unstructured, larger changes would be tolerated.

The control cable at the TM2′-AS1′ junction becomes more $\alpha$-helical and rigid in the AH state, and this appears to be related to the observation that TM2′ helix can continue with AS1′ helix more smoothly as if they were in a single long helix (Fig. 3, *b* and *c*). In other words, the helical axes of TM2′ and AS1′ become well aligned to be connected by virtue of TM2′ bending and transversal move of Trp-209′, as discussed above. Due to this conformational change near the control cable, the N-terminus of AS1 and AS1′ in HAMP comes closer to each other in the AH state (Fig. 3, *b* and *c*). This transversal movement of the control cable, together with the longitudinal displacement discussed above, results in the sliding of the AS1′ helix along the helix axis relative to AS1 by a half helix turn, which subsequently changes the side chain packing at the AS1-AS1′ interface, as shown in Fig. 3 *c* and Fig. 4, *a* and *b*. The change from symmetric packing of the HAMP side chains in the AA state to asymmetric packing in AH can also be verified by analyzing the distances of interacting residue pairs, as summarized in Table S6.

## Ligand occupation induces changes in the HAMP structure and dynamics

Superimposition of the average AA and AH structures with the NMR structure of Af1503 HAMP shows that the NMR structure is closer to the AA structure than the AH structure (Fig. 5, *b* and *c*); the root mean-square deviation differences are summarized in Table S7. A recent study based on the crystal structure of the HAMP domain from *Pseudomonas aeruginosa* (18) suggests that a structure similar to the

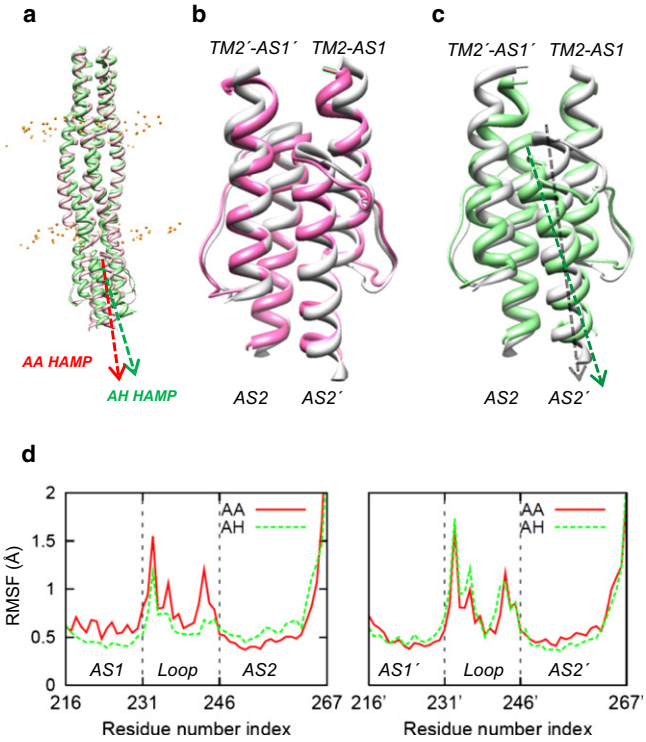


FIGURE 5 (*a*) HAMP domain structures in the AA state (*pink*) and the AH state (*green*) show a change in the HAMP orientation. The HAMP structures are compared with the NMR structure of Af1503 HAMP (*white*) in *b* and *c*. (*d*) $C_\alpha$ RMSF of the HAMP domain, averaged over three independent simulations, are compared in between the AA and AH states for ligand-free monomer (*left*) and for ligand-bound monomer (*right*). In this plot, the RMSF within the HAMP domain are obtained by superimposing the HAMP domain structures to exclude the effect of the whole domain motion. In the left panel of *d*, the RMSF for the AH state becomes smaller at AS1 but larger at AS2 compared to AA, implying that the HAMP helix connected to TM (AS1) becomes less dynamic but the HAMP helix connected to the cytoplasmic domain (AS2) becomes more dynamic upon ligand binding. As a comparison, the RMSF for the ligand-bound monomer shows little difference between the two states, as shown on the right in *d*.

NMR structure of Af1503 HAMP represents either the ligand-on (AH) or ligand-off (AA) state. Our simulation suggests that the NMR structure is closer to the AA state of the Tar HAMP domain.

The following two major structural changes in HAMP are observed: changes in the HAMP domain orientation and in the AS2 orientation. The HAMP domain exhibits more tilting (with less fluctuations) with respect to the membrane normal upon ligand binding (AH) (see Fig. 5 *a* and Fig. S10). The AS2 helix is also more tilted with respect to the axis of HAMP in the ligand-on state (Fig. 5, *b* and *c*, and Fig. S11). This change is caused by the change in the packing at the AS1-AS1′ interface discussed above. In the AH state, the AS2 helix is loosely packed, in contrast to that in the NMR structure, and the AS2 residues show increased fluctuations, as shown in the RMSF plots in Fig. 5 *d*. We note that the cytoplasmic domain helices connected to AS2 are not included in the simulations, and this could affect HAMP dynamics. However, most residues in AS2 remain relatively stable with low RMSF except for several (at most five) terminal residues, suggesting that the overall dynamics of AS2 is not largely affected without the cytoplasmic domain. These two major conformational changes in HAMP are intimately related to the suggestions made from previous experiments (1,14) that ligand binding makes the HAMP region less dynamic and the cytoplasmic domain adjacent to HAMP more dynamic. Our simulation shows similar results with this suggestion in that the global orientation of the HAMP domain becomes less dynamic by attractant binding while the AS2 helix connected to the cytoplasmic domain becomes more dynamic.

## Conformational change of the TM domain induced by ligand binding is correlated with its intrinsic dynamics

Protein conformational change can often be inferred from its intrinsic dynamics. To examine the intrinsic flexibility of the Tar receptor, the principal component analysis (PCA) of the MD simulation trajectories was performed using the GROMACS package, and the most conserved principal modes were selected from each of the three independent simulations for both AA and AH states. These modes are referred to as major modes. Similarities among the three major modes is >0.7 for both AA and AH. The overall motions of AA and AH are similar to each other, and the two subunits TM2 and TM2′ move in the opposite direction in both AA and AH states, resulting in an asymmetric movement (Fig. S12). Fig. S12 *B* shows that the longitudinal motion is the strongest at the periplasmic region, becomes weaker in the bilayer center, and recovers at the control cable. This series of intrinsic motions across the membrane resembles the aforementioned conformational change induced by ligand binding. This PCA analysis clearly shows that the conformational change related to function is correlated with the intrinsic dynamics of the protein. The detailed internal change of the HAMP domain is not clearly seen from PCA, probably due to delicate atomic interactions in the HAMP domain.

## A summary on the conformational changes involved in Tar signaling

Our MD simulations in explicit lipid bilayers have revealed insights into the conformational changes involved in Tar transmembrane signaling. The molecular mechanism based on the simulations involves successive changes from the periplasmic domain to the HAMP domain (Fig. 6): piston displacement of TM2′ at the periplasmic interface, TM2′ bending at the bilayer center, conformational change in the control cable at the TM2′-AS1′ junction, and AS2 tilting that leads to an asymmetric packing and increased dynamics of AS2. This detailed molecular picture is clearly distinguished from a simple mechanical movement of TM2′ as previously suggested (8,9). As discussed above, the conformational/orientational changes can be explained in terms of the interactions between Tar subunits and between Tar and lipids at the atomic level. Therefore, it can be inferred that the amino acid sequence of Tar in the TM domain is a sophisticated design for transmembrane signaling.

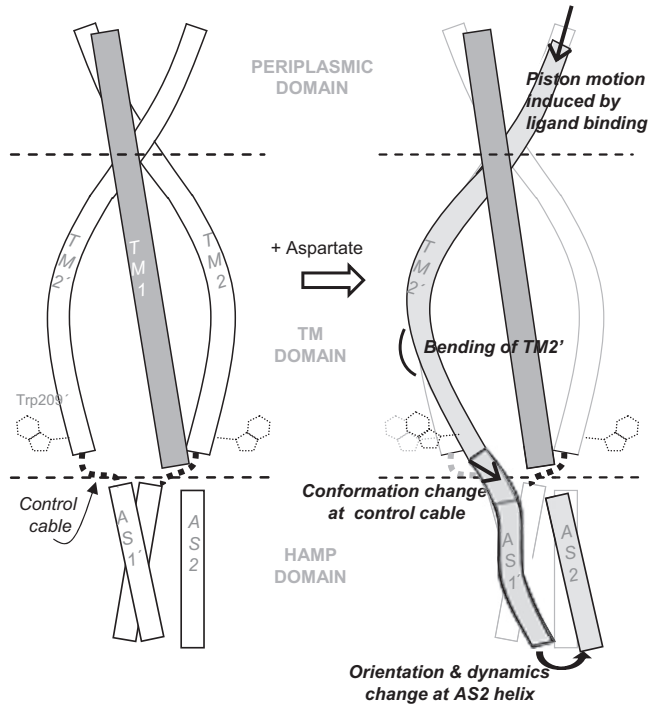


FIGURE 6 Proposed transmembrane signaling mechanism induced by attractant stimulus of aspartate binding in Tar is shown schematically. Piston movement in the periplasmic domain is relayed along the TM2′ helix, bringing about bending of TM2′ at the bilayer center and conformational change at the control cable, and finally induces orientation and dynamics change of HAMP AS2 helix, which would further affect conformational change of the cytoplasmic domain.

### The observed conformational changes are consistent with previously suggested models on signal modulation by HAMP

Several hypothetical models for signal modulation by HAMP have been suggested based on previous experimental results (13–15). On the basis of the analysis of coiled-coil packing patterns in the NMR structure of Af1503 HAMP, Hulko and co-workers suggested a gearbox model in which a concerted rotation of the HAMP helices is involved in signaling. However, this model has been called into question by later studies (8,18). In our simulations, no evidence of HAMP helix rotation was detected, implying that such motion may not be a major contributor to the signal transduction.

The dynamic bundle model (14) is most consistent with our simulation results. In this model, the inward piston motion of TM2′ on the cytoplasmic side weakens the tension exerted on the HAMP domain by the control cable, and HAMP becomes less dynamic, whereas the N-terminus of the cytoplasmic domain connected to HAMP AS2 becomes more dynamic. Surprisingly, this entire picture is well reproduced in our simulation, as described in detail in the previous sections, except that the control cable strengthens the tension exerted on the HAMP domain instead of weakening by attractant binding. However, our MD result does not seem to be at odds with the model, because their description about the control cable is purely based on their intuition, although their description about dynamics of Tar subunits is supported by experimental data. In addition, our trajectory analysis provides details of atomic interactions responsible for the dynamics change in the consecutive domains adjacent to the HAMP domain.

An alternative model suggests a scissor-like movement of the AS2/AS2′ helices of HAMP in response to the piston displacement of the TM2′ helix (15). This model was supported by the x-ray structure of HAMP from *P. aeruginosa* (18), which shows a symmetric orientation change of the AS2/AS2′ helices, compared to the NMR structure. In light of our simulation results, it is our view that this model may be compatible with the aforementioned dynamic bundle model in that the orientation change of the AS2 helix is coupled with the dynamics change in this helix.

### Molecular basis of the negative cooperativity of ligand binding

Finally, the present simulation study allows us to provide the molecular basis for the negative cooperativity of ligand binding to Tar and other chemoreceptors. Ligands usually bind to a single binding site of the homodimer receptors to initiate signaling. As discussed above, the major intrinsic motion favored by the Tar structure is asymmetric (Fig. S12), and the dynamics change in HAMP AS2 occurs due to the asymmetric side chain packing at the AS1-AS1′ interface induced by the asymmetric piston motion (Figs. 3 and 5). The observed important events for signaling are all based on asymmetric interactions/motions and thus may not be promoted by symmetric binding of ligands.

## CONCLUSIONS

All-atom models including the modeled TM domain of chemotaxis receptor Tar were built in explicit lipid bilayers, and further MD simulations were carried out to elucidate the conformational changes induced by ligand binding. Two states representing the ligand-on and -off states were simulated independently and compared with each other. Although the two states share the overall structural architecture, there are small but significant changes around the key residues known to be involved in Tar transmembrane signaling. Notably, many observations are in agreement with various previous experiments including flanking tryptophan residues and flexibility change of the control cable and the HAMP domain.

From the trajectory analysis, we have proposed a mechanistic picture of the transmembrane signaling of Tar across the membrane from the periplasmic domain to the HAMP domain with detailed atomic interactions. The TM2′ helix undergoes an asymmetric piston movement upon ligand binding, and the motion is interpreted into a combination of longitudinal and transversal movements near the cytoplasmic interface by optimal protein-lipid interactions. The rigidity of the control cable is directly influenced by such changes, and the HAMP domain itself becomes rigid but the AS2 helix connected to the cytoplasmic domain becomes more flexible. Previously suggested dynamic bundle model for the transmembrane signaling is very similar to the current simulation results. Moreover, the negative cooperativity of ligand binding can also be explained in terms of the asymmetric motions/dynamics of Tar.

Although comparative long MD simulations were carried out to improve the conformational sampling and to cross-validate the simulation findings, this study may still possess the probability of insufficient sampling. Furthermore, our simulations do not contain the long cytoplasmic domain, a final destination in Tar transmembrane signaling, which makes it hard to draw a complete molecular picture of signal transmission to the cytoplasmic domain via the observed HAMP motion. Nonetheless, good agreement with available experimental information supports our proposed signaling mechanism, and the insightful observations and suggestions made in this work may be verified and enriched by future experiments.

## SUPPORTING MATERIAL

Twelve figures and seven tables are available at http://www.biophysj.org/biophysj/supplemental/S0006-3495(11)00600-X.

This work was supported by the Ministry of Education, Science and Technology (MEST)/Korea Science and Engineering Foundation (KOSEF)

grant No. 305-20100007 (to C.S.), Center for Marine Natural Products and Drug Discovery (CMDD), one of the MarineBio21 programs funded by the Ministry of Land, Transport, and Maritime Affairs of Korea (to H.P.), and National Institutes of Health R01-GM092950 (to W.I.).

## REFERENCES


1. Parkinson, J. S. 2010. Signaling mechanisms of HAMP domains in chemoreceptors and sensor kinases. *Annu. Rev. Microbiol.* 64:101–122.
2. Blair, D. F. 1995. How bacteria sense and swim. *Annu. Rev. Microbiol.* 49:489–522.
3. Baker, M. D., P. M. Wolanin, and J. B. Stock. 2006. Signal transduction in bacterial chemotaxis. *Bioessays.* 28:9–22.
4. Hazelbauer, G. L., and W.-C. Lai. 2010. Bacterial chemoreceptors: providing enhanced features to two-component signaling. *Curr. Opin. Microbiol.* 13:124–132.
5. Murphy, 3rd, O. J., F. A. Kovacs, …, L. K. Thompson. 2001. Site-directed solid-state NMR measurement of a ligand-induced conformational change in the serine bacterial chemoreceptor. *Biochemistry.* 40:1358–1366.
6. Chervitz, S. A., and J. J. Falke. 1996. Molecular mechanism of transmembrane signaling by the aspartate receptor: a model. *Proc. Natl. Acad. Sci. USA.* 93:2545–2550.
7. Lee, G. F., M. R. Lebert, …, G. L. Hazelbauer. 1995. Transmembrane signaling characterized in bacterial chemoreceptors by using sulfhydryl cross-linking in vivo. *Proc. Natl. Acad. Sci. USA.* 92:3391–3395.
8. Draheim, R. R., A. F. Bormans, …, M. D. Manson. 2006. Tuning a bacterial chemoreceptor with protein-membrane interactions. *Biochemistry.* 45:14655–14664.
9. Miller, A. S., and J. J. Falke. 2004. Side chains at the membrane-water interface modulate the signaling state of a transmembrane receptor. *Biochemistry.* 43:1763–1770.
10. Falke, J. J., and G. L. Hazelbauer. 2001. Transmembrane signaling in bacterial chemoreceptors. *Trends Biochem. Sci.* 26:257–265.
11. Ottemann, K. M., W. Xiao, …, D. E. Koshland, Jr. 1999. A piston model for transmembrane signaling of the aspartate receptor. *Science.* 285:1751–1754.
12. Yeh, J. I., H. P. Biemann, …, S. H. Kim. 1996. High-resolution structures of the ligand binding domain of the wild-type bacterial aspartate receptor. *J. Mol. Biol.* 262:186–201.
13. Hulko, M., F. Berndt, …, M. Coles. 2006. The HAMP domain structure implies helix rotation in transmembrane signaling. *Cell.* 126:929–940.
14. Zhou, Q., P. Ames, and J. S. Parkinson. 2009. Mutational analyses of HAMP helices suggest a dynamic bundle model of input-output signalling in chemoreceptors. *Mol. Microbiol.* 73:801–814.
15. Swain, K. E., M. A. Gonzalez, and J. J. Falke. 2009. Engineered socket study of signaling through a four-helix bundle: evidence for a yin-yang mechanism in the kinase control module of the aspartate receptor. *Biochemistry.* 48:9266–9277.
16. Biemann, H. P., and D. E. Koshland, Jr. 1994. Aspartate receptors of *Escherichia coli* and *Salmonella typhimurium* bind ligand with negative and half-of-the-sites cooperativity. *Biochemistry.* 33:629–634.
17. Yang, Y., H. Park, and M. Inouye. 1993. Ligand binding induces an asymmetrical transmembrane signal through a receptor dimer. *J. Mol. Biol.* 232:493–498.
18. Airola, M. V., K. J. Watts, …, B. R. Crane. 2010. Structure of concatenated HAMP domains provides a mechanism for signal transduction. *Structure.* 18:436–448.
19. Swain, K. E., and J. J. Falke. 2007. Structure of the conserved HAMP domain in an intact, membrane-bound chemoreceptor: a disulfide mapping study. *Biochemistry.* 46:13684–13695.
20. Peach, M. L., G. L. Hazelbauer, and T. P. Lybrand. 2002. Modeling the transmembrane domain of bacterial chemoreceptors. *Protein Sci.* 11:912–923.
21. Kandt, C., W. L. Ash, and D. P. Tieleman. 2007. Setting up and running molecular dynamics simulations of membrane proteins. *Methods.* 41:475–488.
22. Anezo, C., A. H. de Vries, …, S.-J. Marrink. 2003. Methodological issues in lipid bilayer simulations. *J. Phys. Chem. B.* 107:9424–9433.
23. Pakula, A. A., and M. I. Simon. 1992. Determination of transmembrane protein structure by disulfide cross-linking: the *Escherichia coli* Tar receptor. *Proc. Natl. Acad. Sci. USA.* 89:4144–4148.
24. Im, W., M. S. Lee, and C. L. Brooks, 3rd. 2003. Generalized born model with a simple smoothing function. *J. Comput. Chem.* 24:1691–1702.
25. Brooks, B. R., C. L. Brooks, 3rd, …, M. Karplus. 2009. CHARMM: the biomolecular simulation program. *J. Comput. Chem.* 30:1545–1614.
26. MacKerel, Jr., A. D., D. Bashford, …, M. Karplus. 1998. All-atom empirical potential for molecular modeling and dynamics studies of proteins. *J. Phys. Chem. B.* 102:3586–3616.
27. Ryckaert, J. P., G. Ciccotti, and H. J. C. Berendsen. 1977. Numerical integration of the cartesian equations of motion of a system with constraints; molecular dynamics of *n*-alkanes. *J. Comput. Phys.* 23:327–341.
28. Canutescu, A. A., A. A. Shelenkov, and R. L. Dunbrack, Jr. 2003. A graph-theory algorithm for rapid protein side-chain prediction. *Protein Sci.* 12:2001–2014.
29. Lindahl, E., B. Hess, and D. van der Spoel. 2001. GROMACS 3.0: a package for molecular simulation and trajectory analysis. *J. Mol. Model.* 7:306–317.
30. Berendsen, H. J. C., J. P. M. Postma, …, J. Hermans. 1981. Interaction models for water in relation to protein hydration. *In* Intermolecular Forces. B. Pullman, editor. Reidel, Dordrecht, Holland. 331–342.
31. Tieleman, D. P., M. S. P. Sansom, and H. J. C. Berendsen. 1999. Alamethicin helices in a bilayer and in solution: molecular dynamics simulations. *Biophys. J.* 76:40–49.
32. van Gunsteren, W. F., and H. J. C. Berendsen. 1987. Gromos-87 manual. *Biomos Bv.* University of Groningen, Netherlands.
33. Berger, O., O. Edholm, and F. Jähnig. 1997. Molecular dynamics simulations of a fluid bilayer of dipalmitoylphosphatidylcholine at full hydration, constant pressure, and constant temperature. *Biophys. J.* 72:2002–2013.
34. Apweiler, R., A. Bairoch, and C. H. Wu. 2004. Protein sequence databases. *Curr. Opin. Chem. Biol.* 8:76–80.
35. Berendsen, H. J. C., J. P. M. Postma, …, J. R. Haak. 1984. Molecular dynamics with coupling to an external bath. *J. Chem. Phys.* 81:3684–3690.
36. Darden, T., D. York, and L. Pedersen. 1993. Particle mesh Ewald an Nlog(N) method for Ewald sums in large systems. *J. Chem. Phys.* 98:10089–10092.
37. Hess, B., H. Bekker, …, J. G. E. M. Fraaije. 1997. LINCS: a linear constraint solver for molecular simulations. *J. Comput. Chem.* 18:1463–1472.
38. Sal-Man, N., D. Gerber, and Y. Shai. 2004. The composition rather than position of polar residues (QxxS) drives aspartate receptor transmembrane domain dimerization *in vivo*. *Biochemistry.* 43:2309–2313.
39. Kachel, K., E. Asuncion-Punzalan, and E. London. 1995. Anchoring of tryptophan and tyrosine analogs at the hydrocarbon-polar boundary in model membrane vesicles: parallax analysis of fluorescence quenching induced by nitroxide-labeled phospholipids. *Biochemistry.* 34:15475–15479.
40. Boldog, T., and G. L. Hazelbauer. 2004. Accessibility of introduced cysteines in chemoreceptor transmembrane helices reveals boundaries interior to bracketing charged residues. *Protein Sci.* 13:1466–1475.
41. Chen, X., and D. E. Koshland, Jr. 1995. The N-terminal cytoplasmic tail of the aspartate receptor is not essential in signal transduction of bacterial chemotaxis. *J. Biol. Chem.* 270:24038–24042.
42. Ames, P., Q. Zhou, and J. S. Parkinson. 2008. Mutational analysis of the connector segment in the HAMP domain of Tsr, the *Escherichia coli* serine chemoreceptor. *J. Bacteriol.* 190:6676–6685.
43. Wright, G. A., R. L. Crowder, …, M. D. Manson. 2011. Mutational analysis of the transmembrane helix 2-HAMP domain connection in the *Escherichia coli* aspartate chemoreceptor tar. *J. Bacteriol.* 193:82–90.